Hindawi
Advances in Condensed Matter Physics
Volume 2021, Article ID 2321558, 12 pages
https://doi.org/10.1155/2021/2321558

Research Article

The Relationship between the Structure and Thermal Properties of Bi_2O_3-ZnO-B_2O_3 Glass System

Sung-Hung Lan,[1] **Chin-Tung Lee**,[2] **Yi-Sheng Lai**,[1,2] **Chien-Chon Chen**,[1] **and Hsi-Wen Yang**[1,2]

[1]*Ph. D. Program in Materials and Chemical Engineering, National United University, 2, Lienda, Miaoli 360001, Taiwan*
[2]*Department of Materials Science and Engineering, National United University, 2, Lienda, Miaoli 360001, Taiwan*

Correspondence should be addressed to Hsi-Wen Yang; hwyang@nuu.edu.tw

Received 9 May 2021; Revised 15 June 2021; Accepted 6 August 2021; Published 21 August 2021

Academic Editor: Ram N. P. Choudhary

The influence of Bi_2O_3 and melting temperature on the thermal and structural properties of xBi_2O_3-(60-x) ZnO-40B_2O_3 glasses has been investigated in this study. It is expected that these factors can be used to control the degree of reduction of Bi_2O_3, and the relationship between these factors and the color change of the process for bismuth glass is discussed. Due to high-temperature melting, the bismuth-doped borate glasses have changed into dark/black from original transparent yellow and the light transmittance will decrease, so it is not used in optical applications. The thermal properties of glass are measured by a thermomechanical analyzer (TMA), and the glass structure is analyzed by FTIR and XPS. The results show that the glass is mainly composed of [BiO_6] octahedron, [BiO_3] triangle, [BO_4] tetrahedron, and triangle [BO_3] units, and the network of the glass system is mainly bonded by B-O-B, B-O-Zn, B-O-Bi, and Bi-O-Bi. The glass thermal expansion coefficient (CTE) of this glass system increases with the increase of Bi_2O_3 content, and the O1*s* nuclear electron binding energy shifts to the lower energy direction with the increase of Bi_2O_3 addition. In terms of FTIR, as the melting temperature rises, the B-O-B bonding vibration concentration of [BO_4] inside the borate glass decreases, and the density of B-O-B bonding vibration of [BO_3] increases, Moreover, the increase in melting temperature increases the probability of reducing Bi ions to Bi^0, reduces the bonding of Bi-O-B, and increases the bonding of B-O-B, and the CTE also slightly decreases.

1. Introduction

Adding PbO to the glass can make the glass have good light transmittance, stable structure, low-temperature glass characteristic temperature, excellent optical properties, thermal properties, and electrical properties [1], but it is easy to cause harmful effects on the environment and the human body. The development of lead-free glass to replace lead-containing glass is the main research direction at present, and the component of lead oxide is bismuth oxide (Bi_2O_3), its Bi^{3+} property is similar to Pb^{2+} of lead oxide (PbO), both have the same electronic configuration and high polarizability [2], and the glass also has low melting temperature, high density, high refractive index, and other characteristics, which can be used to replace lead oxide to develop various lead-free glass products [3, 4]; therefore, bismuth glass is one of the most promising glasses without considering the lead-containing glass [5, 6].

Dietzel [7] derived the Coulomb electrostatic force field and field strength formula in 1942 and pointed out that the structure of borate glass [BO_3] is a plane triangle, and the boron coordination number is 3. If an additional free oxygen atom is provided, BO_3 can bond with the oxygen atom to form a BO_4 tetrahedral with a coordination number of 4. [BO_3] and [BO_4] are usually connected in a ring in glass, which is called a boron ring structure (boroxol group structure), a random network structure formed by bonding with B-O-B. In the cation field strength theory of glass structure theory, because the field strength of Bi_2O_3 is weak, it belongs to the nature of glass as an intermediate agent and

cannot form glass alone. Adding Bi_2O_3 to ZnO, SiO_2, B_2O_3, and other materials can help the glass network to be more stable and promote the formation of glass structures. S. Bale, T. Maeder, and other authors [8–11] stated, respectively, that the glass intermediate Bi_2O_3 is sometimes presented as $[BiO_3]$ and $[BiO_6]$ structural units in the glass structure or as $[BiO_3]$ triangles or $[BiO_6]$ octahedron and other structural units appear, and Bi_2O_3 can be used as a glass modifier or glass forming agent, depending on the proportion of Bi_2O_3 in the overall glass composition.

As for the coloring phenomenon of bismuth glass, Saitoh et al. [12] and other scholars pointed out that the electronic structure of coloring is related to the Bi valence, originating from Bi^{3+} and Bi^{5+}, and/or plasma Bi^0 clusters in colored glass, because Bi^{3+}, the energy bandgap of the transition state in the s–p orbital domain between 3.6 and 4.7 eV, is the optical band gap and the visible absorption band between 2.5 and 2.7 eV, which is related to the coloring phenomenon, the ionic reduction behavior of bismuth glass. Gerth and Russel [13] pointed out that in the Bi_2O_3-TiO_2-B_2O_3 glass system the Bi_2O_3 glass increases both the Bi_2O_3 content and the melting temperature, which causes the glass to change from light yellow to brownish-black gradually. Because Bi^{3+} is easily reduced to Bi^{2+}, Bi^{+}, and Bi^0 [14, 15], the reduction reaction can be strengthened with the increase of melting temperature and Bi_2O_3 content, which make the color of the glass deep, and the light transmittance decreases [14].

2. Materials and Methods

In this study, x Bi_2O_3-(60-x) ZnO-40 B_2O_3 ($x = 10$, 20, 30), where $40B_2O_3$ is a fixed component, changes $x = Bi_2O_3$ content at different melting temperatures (900°C, 1000°C, 1100°C, and 1200°C), to explore the influence of bismuth oxide content change and melting temperature change on its structure. The use of reagent grade B_2O_3 (JT Baker, 99.9%), ZnO (JT Baker, 99.7%), and Bi_2O_3 (Sigma-Aldrich, 98%) as the raw material of glass is configured into the following glass component series and melted at the process temperature of 900°C, 1000°C, 1100°C, and 1200°C:

A1: 10 Bi_2O_3-50 ZnO-40 B_2O_3

A2: 20 Bi_2O_3-40 ZnO-40 B_2O_3

A3: 30 Bi_2O_3-30 ZnO-40 B_2O_3

In the experiment, the required weight of each raw material was calculated according to the molar fraction of the composition, and the raw material powder was mixed into 30 g. After the prepared raw materials are uniformly mixed, they were put into an alumina crucible, melted in an electric furnace at a heating rate of 10°C per minute, heated to different process temperatures, and kept at a constant temperature for 1.5 hours to promote uniform mixing of the glass. The molten glass is taken out of the high-temperature electric furnace and cast on a stainless steel plate preheated to the annealing temperature, in order to eliminate the thermal stress caused by the rapid cooling of the glass, and the glass must be immediately sent to the annealing furnace and slowly cooled down to room temperature.

X-ray diffraction analysis uses Rigaku Rint 2200 type and uses CuKa as the diffraction light source and the filter as Ni filter, the operating voltage is 30 kV, and the current is 20 mA. The scanning speed is set to 8 degrees per minute for analysis, and the finished glass is analyzed by X-ray diffraction (XRD) to confirm that there is no crystal in the glass. Fourier-transform infrared (FTIR) spectroscopy (Perkin Elmer, USA) was used for analysis, and it was carried out at room temperature. The glass powder to be measured was placed in the alumina grind, with a concentration of 1wt % of optical grade KBr powder, and mixed and ground evenly in the bowl, and about 500 mg of the mixed powder was taken, pressed into a translucent round sheet, and then tested. The range of test wavenumber is 450~2000 cm^{-1}. Through the XPS spectroscopic analysis, the glass test piece is ground into powder and analyzed by a X-ray photoelectron spectrometer. Experimental parameters are as follows: source type: Al K alpha, spot size: 400 μm, analyzer mode: CAE, and pass energy: 50.0 eV. We obtain the O1*s* and Bi4*f* XPS lines of each sample and analyze the peaks of the XPS line components. TMA, the thermal mechanical analyzer, is the most used to measure the coefficient of thermal expansion (CTE), which is the average value of the thermal strain versus the temperature change after a material passes through a temperature change curve. The thermal analysis of the glass in this experiment uses a thermomechanical analyzer Perkin Elmer TMA 7, USA. The glass sample was ground into a square test piece with a size of $5 \times 5 \times 5$ (mm) parallel to the top and bottom and placed in the carrier of the TMA instrument at a heating rate of 10°C per minute.

3. Results and Discussion

3.1. XRD Diffraction Analysis. A series of glass samples were analyzed by XRD diffraction. In the analysis chart, glass samples such as A1, A2, and A3 were melted at 900°C, 1000°C, 1100°C, and 1200°C, respectively, and all 12 samples were with hump characteristic of typical amorphous materials, without any crystal diffraction peaks, so it can be confirmed that the sample has no crystals. As the amorphous material is a disordered material, the hump, or the second broad hump at the higher incidence angle of XRD, is an indication of the disordered state. When the content of Bi_2O_3 increases, indicating a second wide hump at higher incidence angles of XRD, the internal structure of the material at this content is also amorphous, as shown in Figure 1.

3.2. FTIR. In FTIR spectroscopy, based on the research of previous literature, there are four characteristic peaks of glass structure in A series glass, such as $[BiO_3]$, $[BiO_6]$, $[BO_3]$, and $[BO_4]$ (Table 1).

In the FTIR spectrum, there are $[BiO_3]$, $[BiO_6]$, Bi–O–Bi, Bi-O^-, and the triangular $[BO_3]$ unit of the borate B_2O_3 glass and the B–O^- unit of the $[BO_4]$ tetrahedron and absorption peak. In Figure 2, it can be roughly divided into 3 blocks: (1) between 510 cm^{-1} and 700 cm^{-1}, it is a three-coordinated plane $[BiO_3]$ and a six-coordinated octahedral $[BiO_6]$

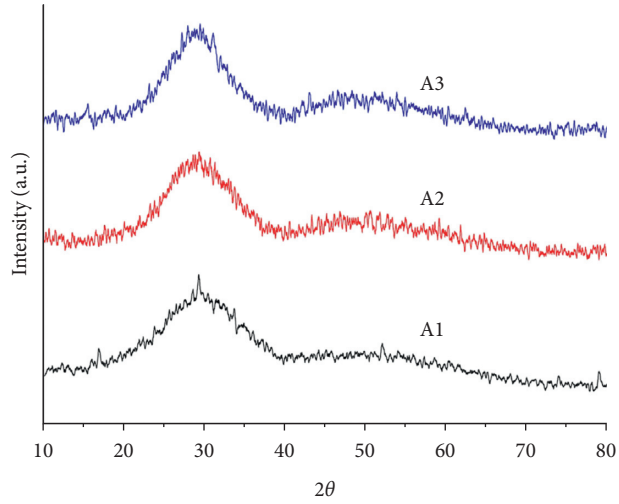

Figure 1: XRD diffraction patterns of A series glass melted test pieces.

Table 1: Corresponding characteristics and bands of each vibration peak of FTIR of A glass series.

Wavenumber (cm^{-1})	Vibrational mode	Reference
510~550	Symmetrical stretching vibration of Bi–O–Bi bond	[1, 6, 16]
600	Symmetrical stretching vibration of the Bi–O–Bi bond	[16–18],
700~716 750~780	B-O bending vibration of [BO_3] structural unit	[16, 19–23]
820 900~950	[BO_4] B–O^- stretching vibration in the unit	[16, 21, 24, 25]
1000 1015–1021	B–O^- stretching vibration of [BO_4] unit	[16, 19, 20, 22, 23]
1250~1310	B–O^- asymmetric stretching vibration of [BO_3] unit	[16, 19, 23, 25]
1365–1472	B–O^- asymmetric stretching vibration of [BO_3] unit	[16, 19, 23]
1635~1650	Bending vibration of OH^- bond	[1, 16, 20]

structural unit; (2) between 700 cm^{-1} and 1382 cm^{-1}, it is a plane triangle [BO_3], and a tetrahedral [BO_4] structural unit is the main one; and (3) between 1382 cm^{-1}~1640 cm^{-1}, the plane triangle [BO_3] and [OH^-] bond is the main part. Among the three blocks, there are 4 absorption characteristic peak locations, 700 cm^{-1}, 777 cm^{-1}, 1382 cm^{-1}, and 1640 cm^{-1}, which are relatively easy to distinguish. And the others are 510 cm^{-1}, 820 cm^{-1}, and 1000 cm^{-1}, where the absorption characteristic peaks are relatively weak.

There is a weak absorption peak at the wavenumber of 510 cm^{-1}, which is the symmetric stretching vibration of the Bi-O-Bi bond in the [BiO_3] and [BiO_6] unit. The absorption peak is located at the wavenumber of about 700 cm^{-1}, which is [BO_3] B-O-B vibration. The absorption peak is located at the wavenumber of about 777 cm^{-1}, which is the absorption peak of B-O-B vibration in the [BO_3] unit. It is the B–O^- stretching vibration of the [BO_4] tetrahedral unit in the glass structure at the wavenumber of 820 cm^{-1}, the wavenumber at 1000 cm^{-1} (solid arrow) is the B–O^- stretching vibration of the [BO_4] tetrahedral unit, and at the wavenumber of about 1382 cm^{-1}, it is the Bi-O^- unit structure in the [BiO_3] structural unit vibration, and the absorption peak at 1640 cm^{-1} is the vibration of the OH radical. In Figure 2, there is a weak absorption peak at the wavenumber of 510 cm^{-1}, the symmetrical stretching vibration of the Bi-O-Bi bond in the [BiO_3] and [BiO_6] units, and the signal is very weak. At 700 cm^{-1} and 777 cm^{-1} (dashed arrow) is the vibration signal of the [BO_3] unit. At 1000°C, 700 cm^{-1} is more obvious, indicating that the [BO_3] structure concentration is high, and the [BO_4] structure concentration is low. At 777 cm^{-1} (dashed arrow), the signal is very weak. At 1382 cm^{-1} absorption peak, the vibration signal of [BO_3] increases as the melting temperature rises, indicating that the structure of the [BO_3] unit rises with the increase in melting temperature. The OH^{-1} vibrates at 1640 cm^{-1}, and the signal is smaller at 900°C, and when the melting temperature rises, then the signal weakens. In Figures 3 and 4, the vibration signals of [BO_3] at 700 cm^{-1} and 777 cm^{-1} (dashed arrow) are stronger than those in Figure 2, indicating that the [BO_3] structure concentration of A2 and A3 is higher, and the [BO_4] structure concentration is low. The signal is very weak at 777 cm^{-1} (dashed arrow). The vibration signal of [BO_3] at 1382 cm^{-1} increases as the melting temperature increases, indicating that the concentration of the [BO_3] structure of A2 and A3 increases as the melting temperature rises, and the [BO_4] structure concentration decreases. Since B-O-B bonding energy > Bi-O-Bi bonding energy, it means that B-O-B bonding of [BO4] unit and

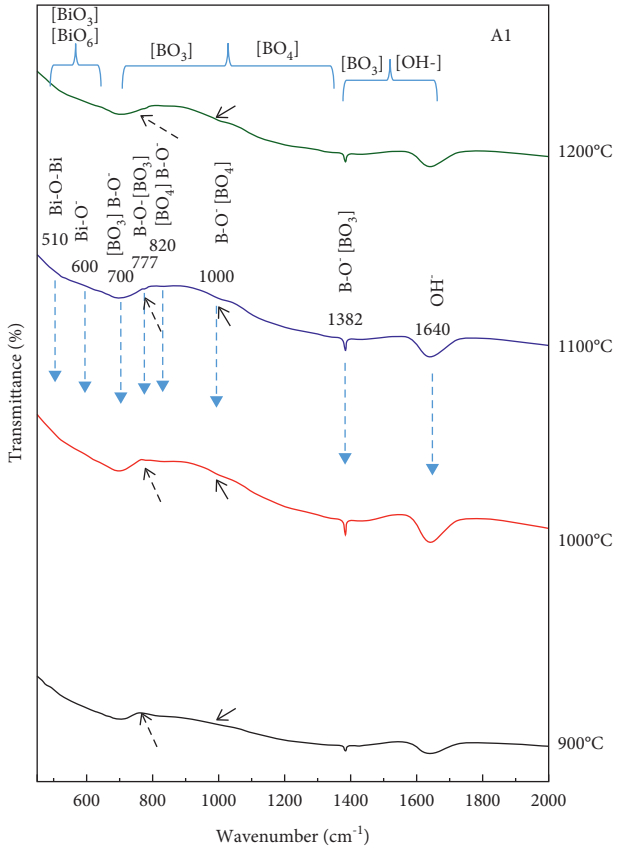

FIGURE 2: FTIR spectra of A1 glass series at different melting temperatures of 900°C, 1000°C, 1100°C, and 1200°C.

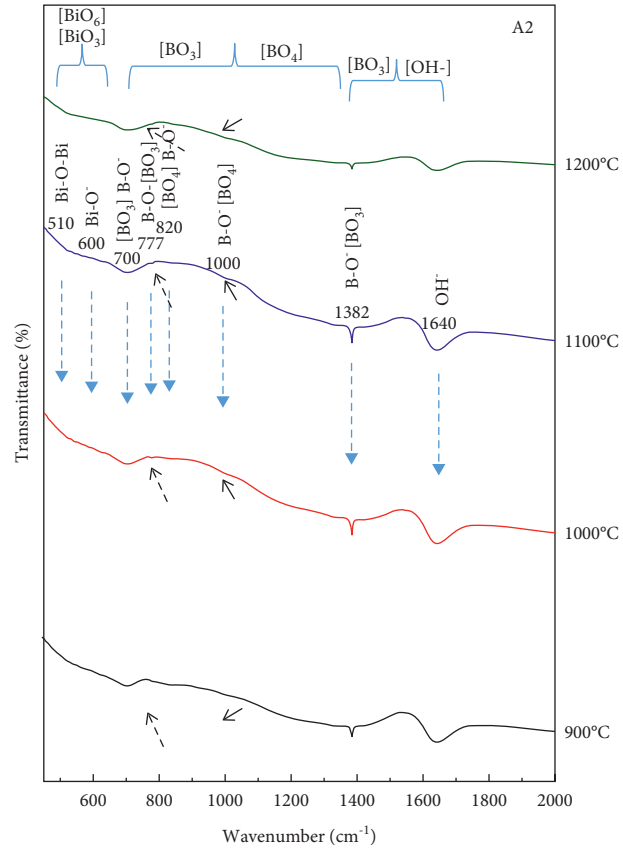

FIGURE 3: FTIR spectra of A2 glass series at different melting temperatures of 900°C, 1000°C, 1100°C, and 1200°C.

Bi-O-Bi bonding will relax and decompose due to high temperature. And based on the energy balance trend of the glass system, this system promoted the gradual formation of the Bi-O-B bond and $[BO_3]$ of the intermediate bond energy.

At 1382 cm^{-1} ($B\text{-}O^-$ bonding vibration of $[BO_3]$ unit), A1, A2, and A3 series glasses all have obvious absorption peaks. As the melting temperature increases, the strength of the absorption peak is as follows:

$$A3_{900°C} > A3_{1000°C} > A3_{1100°C} > A3_{1200°C}$$
$$A2_{1100°C} > A2_{1000°C} > A2_{900°C} > A2_{1200°C}$$
$$A1_{1000°C} > A1_{1100°C} > A1_{1200°C} > A1_{900°C}$$

In the A3 glass series, because the 30 mol % of Bi_2O_3 content is relatively high, it has a relatively sufficient reaction concentration with $[BO_3]$ and $[BO_4]$ unit, so it is clearly observed that as the melting temperature increases, the concentration of $B\text{-}O^-$ of $[BO_3]$ unit decreases. And A1, A2, and A3 glass systems all tend to shift to high wavenumbers. This shift phenomenon is that as the melting temperature rises, Bi^{3+} is reduced to low-valent ions and partly reduced to Bi^0 to dissolve and causes the glass color to be darker brown, and when the melting temperature rises, the B-O-B content of $[BO_4]$ in the original borate glass decreases, and the B-O-B concentration of $[BO_3]$ unit increases. Since the B-O-B bond energy is greater than B-O-Bi, the bond length of B-O-B is shorter than that of B-O-Bi; therefore, it tends to move toward a high wavenumber.

In Figure 5(a), at a melting temperature of 900°C and a wavenumber of 1382 cm^{-1} ($B\text{–}O^-$ in the $[BO_3]$ unit), as the concentration of Bi_2O_3 increases, the signal of $B\text{–}O^-$ in the $[BO_3]$ unit increases, showing that the tetrahedral $[BO_4]$ structure is loosened and dissociated, providing oxygen atoms for Bi_2O_3 bonding, and the tetrahedral $[BO_4]$ structure is transformed into a triangle $[BO_3]$, so the signal of $B\text{–}O^-$ in the $[BO_3]$ unit is enhanced. Between 1000 cm^{-1} (solid arrow) and 1382 cm^{-1}, it has a tetrahedral $[BO_4]$ structure. It can be observed that as the concentration of Bi_2O_3 increases, the signal of $B\text{–}O^-$ in the $[BO_4]$ unit decreases, indicating that the network of the $[BO_4]$ unit of the structure drops. With the increase of Bi_2O_3 concentration, $[BiO_3]$ tends to gradually become the glass network formers of A series glass. Furthermore, from the FTIR diagram, it can be clearly judged that the Bi-O bond strength is less than the B-O bond strength, resulting in the glass structure network connection; the strength is, therefore, weakened at the same time, which causes the CTE to increase with the increase of Bi_2O_3 concentration. Because of the high polarizability of bismuth ions in high-content bismuth oxide glass, the octahedron $[BiO_6]$ produces serious distortion and deformation, so the glass structure, a low-coordination $[BiO_3]$ and bismuth-oxygen trigonal bismuth ion, is formed [11].

Therefore, in the FTIR analysis, the structural system can be determined. As the concentration of Bi_2O_3 increases, the characteristic absorption peak intensity of the tetrahedral

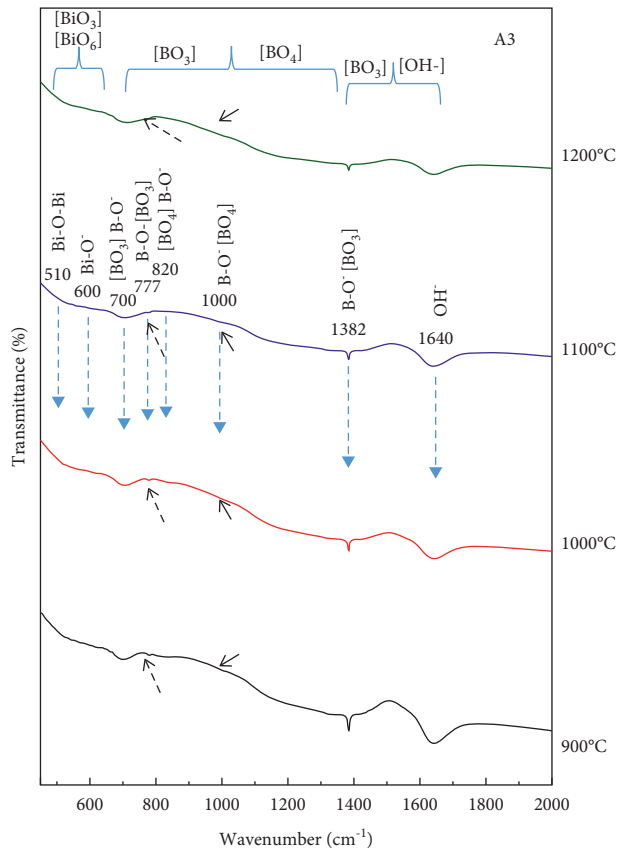

Figure 4: FTIR spectra of A3 glass series at different melting temperatures of 900°C, 1000°C, 1100°C, and 1200°C.

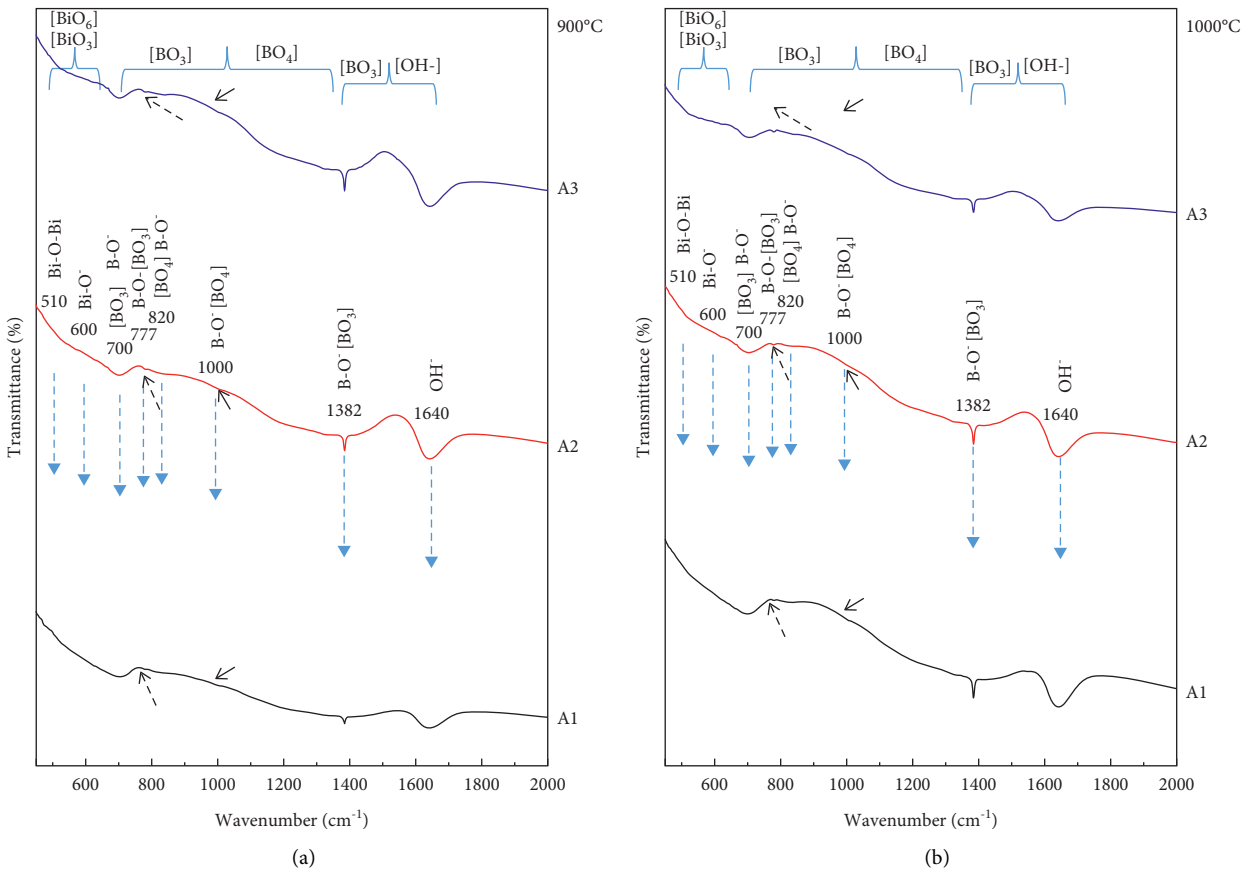

Figure 5: Continued.

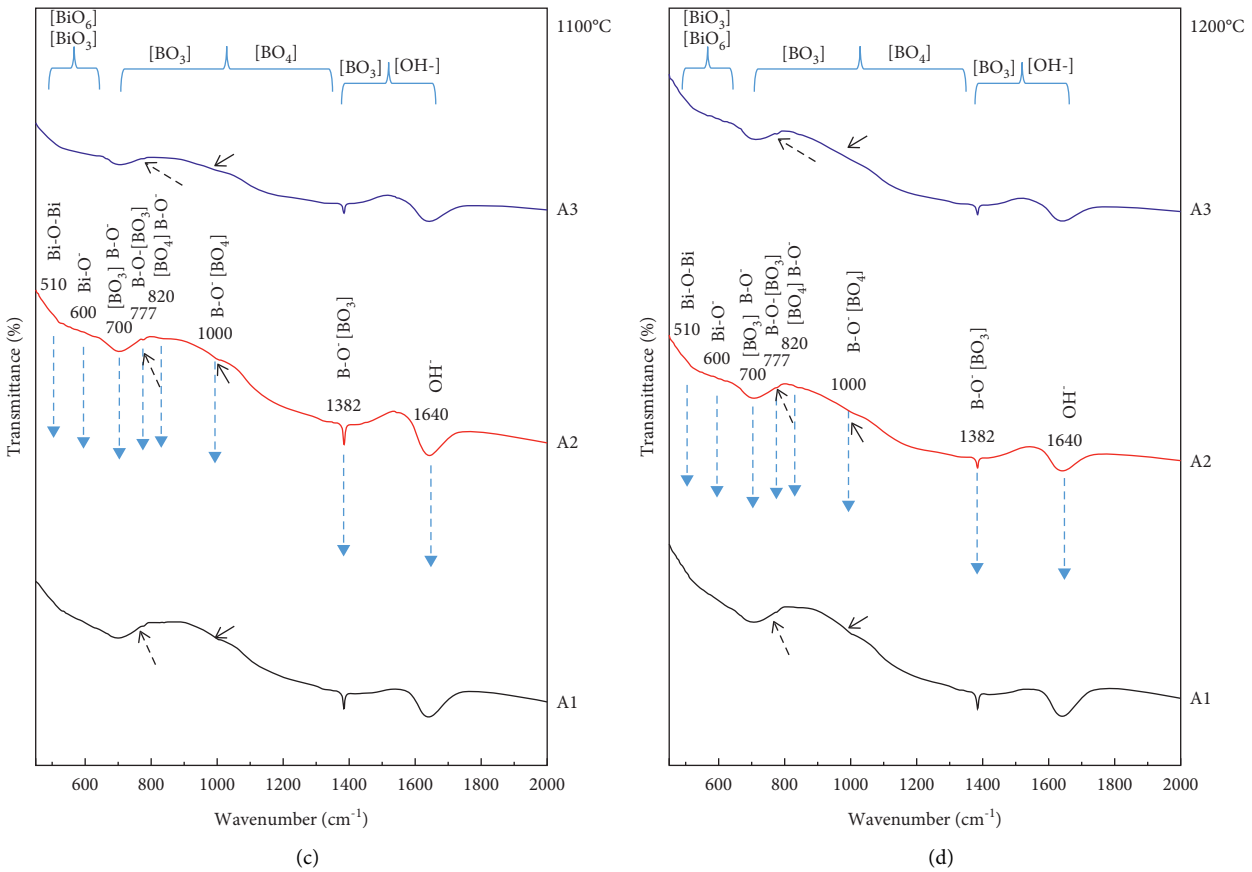

Figure 5: FTIR spectra of A series at different melting temperatures of 900°C, 1000°C, 1100°C, and 1200°C.

$[BO_4]$ structural unit weakens, and the $[BO_3]$ structural unit forms a chain or ring with the B-O-B bond of polyborate. The intensity of characteristic absorption peaks of trigonal $[BO_3]$, $[BiO_3]$, and $[BiO_6]$ structural units has been enhanced.

3.3. XPS. In the A glass series, Figure 6 shows O1*s* spectra of melting at different temperatures of 900°C, 1000°C, 1100°C, and 1200°C. At 900°C, $A1 = 530.85$ eV, $A2 = 530.5$ eV, and $A3 = 530.39$ eV; the same is true at 1000°C, 1100°C, and 1200°C. As the content of Bi_2O_3 increases, the binding energy of the $O1_s$ spectrum all shifts to the lower binding energy direction, which is consistent with the observation results of FTIR.

In Figure 7, with the increase of melting temperature, the binding energy of O1*s* energy spectrum of A1, A2, and A3 series glass is observed, except at 1200°C; the others are all shifting to the lower binding energy direction, which is consistent with the observation results of FTIR.

Figure 8 shows the spectra of Bi4$f_{7/2}$ and Bi4$f_{5/2}$-XPS melted at 900°C, 1000°C, 1100°C, and 1200°C for A1, A2, and A3 series glasses, respectively. The binding energy range is from 155 eV to 170 eV. The former is Bi4$f_{7/2}$(eV) and the latter is Bi4$f_{5/2}$(eV) signals [26, 27], located at 156.2 eV, 158.9 eV, 159.5 eV, and 161 eV which are the binding energies of Bi^0, Bi^{+1}, Bi^{+2}, Bi^{3+}, and Bi^{5+} ions of Bi4$f_{7/2}$, respectively [27], and Bi^0, Bi^{+1}, Bi^{+2}, Bi^{3+}, and Bi^{5+} ions binding energy at 162.1 eV, 164 eV, 165 eV, and 166 eV are Bi4$f_{5/2}$, respectively [27].

Observing Figure 8, it can also be clearly seen that when the Bi_2O_3 concentration is 20 mol %, the Bi^{3+} and Bi^{5+} ion concentrations of Bi4$f_{7/2}$ in the A1, A2, and A3 glass systems decrease, and the Bi^{+1} and Bi^{+2} ion concentrations increase. As the Bi^0 concentration signal increases, bismuth ions tend to be reduced to Bi^0, and the structure gradually forms a glass unit structure dominated by $[BiO_3]$, $[BiO_6]$, $[BO_3]$, and $[BO_4]$. With the increase in melting temperature, Bi^{3+} ions can obtain additional heat energy and will also be reduced. Bi ions of different valences, $Bi^{3+} \longrightarrow Bi^{+1}$, Bi^{+2}, or Bi^0 are precipitated. As the melting temperature rises, the Bi ions are dissolved in the glass easily bond with other atoms in the system to form Bi-O-B and Bi-O-Zn bonded glass structures. Figure 6 shows the XPX-$O1_s$ spectra of A series glass melted at different temperatures of 900°C, 1000°C, 1100°C, and 1200°C. As the content of Bi_2O_3 increases, the binding energy of $O1_s$ spectrum shifts to the direction of lower binding energy, showing that the high-strength bonds will gradually decompose and in turn will form more lower-strength $[BO_3]$, $[BiO_3]$, and $[BiO_6]$ bonds, and the overall glass structure will become looser.

Figure 9 shows the Bi4$f_{7/2}$ and Bi4$f_{5/2}$ energy spectra for (a) A1 glass, (b) A2 glass, and (c) A3 glass at different melting temperatures of 900°C, 1000°C, 1100°C, and 1200°C. As the

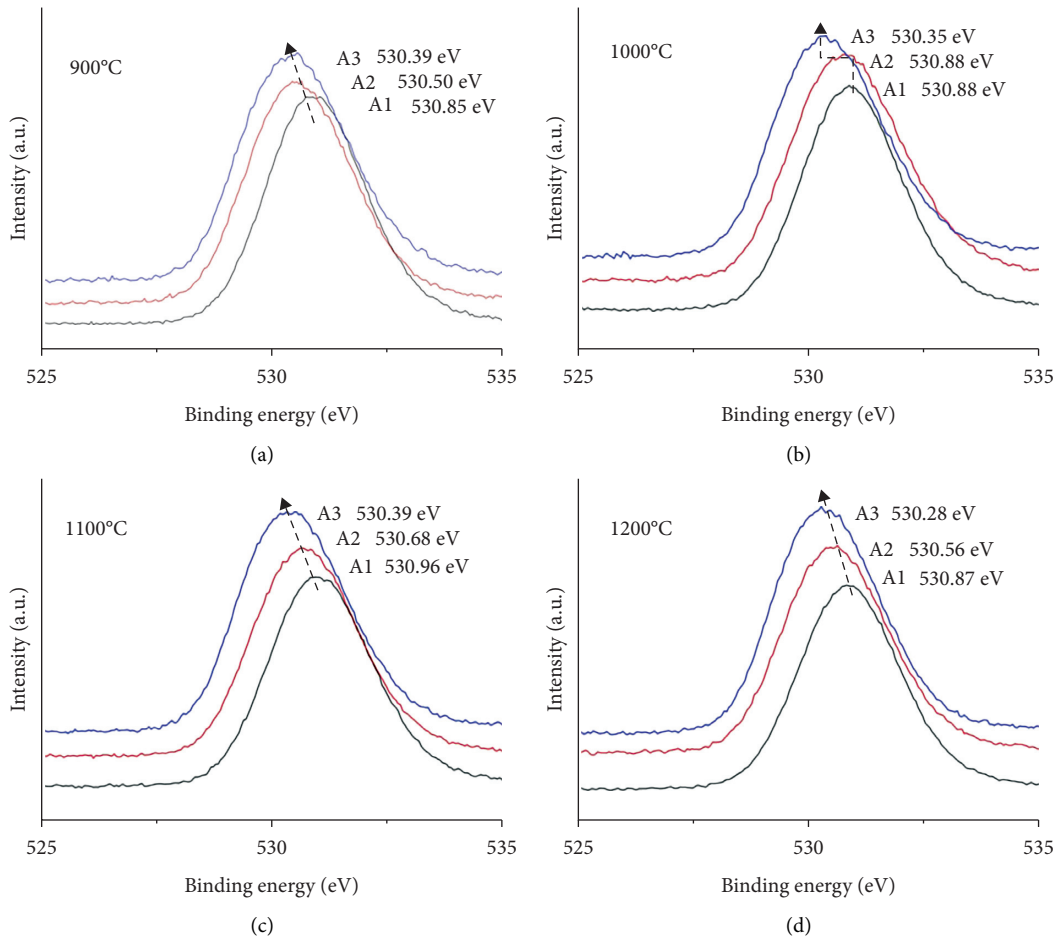

Figure 6: XPS-O1*s* spectra of A series glass melted at different temperatures of 900°C, 1000°C, 1100°C, and 1200°C.

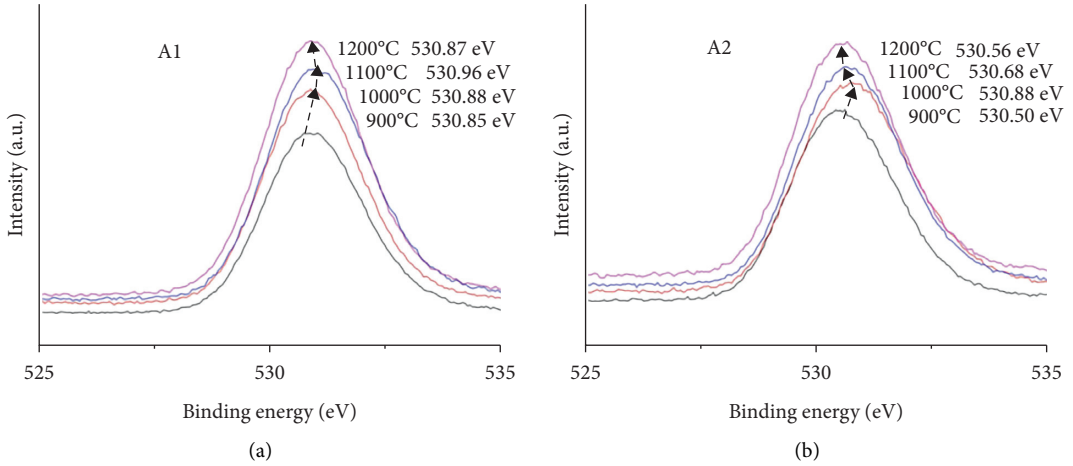

Figure 7: Continued.

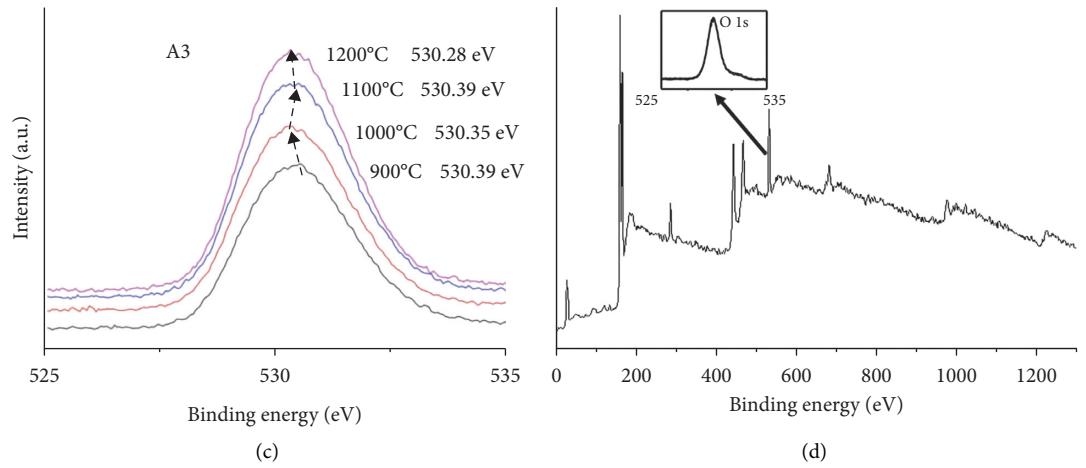

Figure 7: O1*s* spectra of A1, A2, and A3 series glasses, respectively, melted at 900°C, 1000°C, 1100°C, and 1200°C.

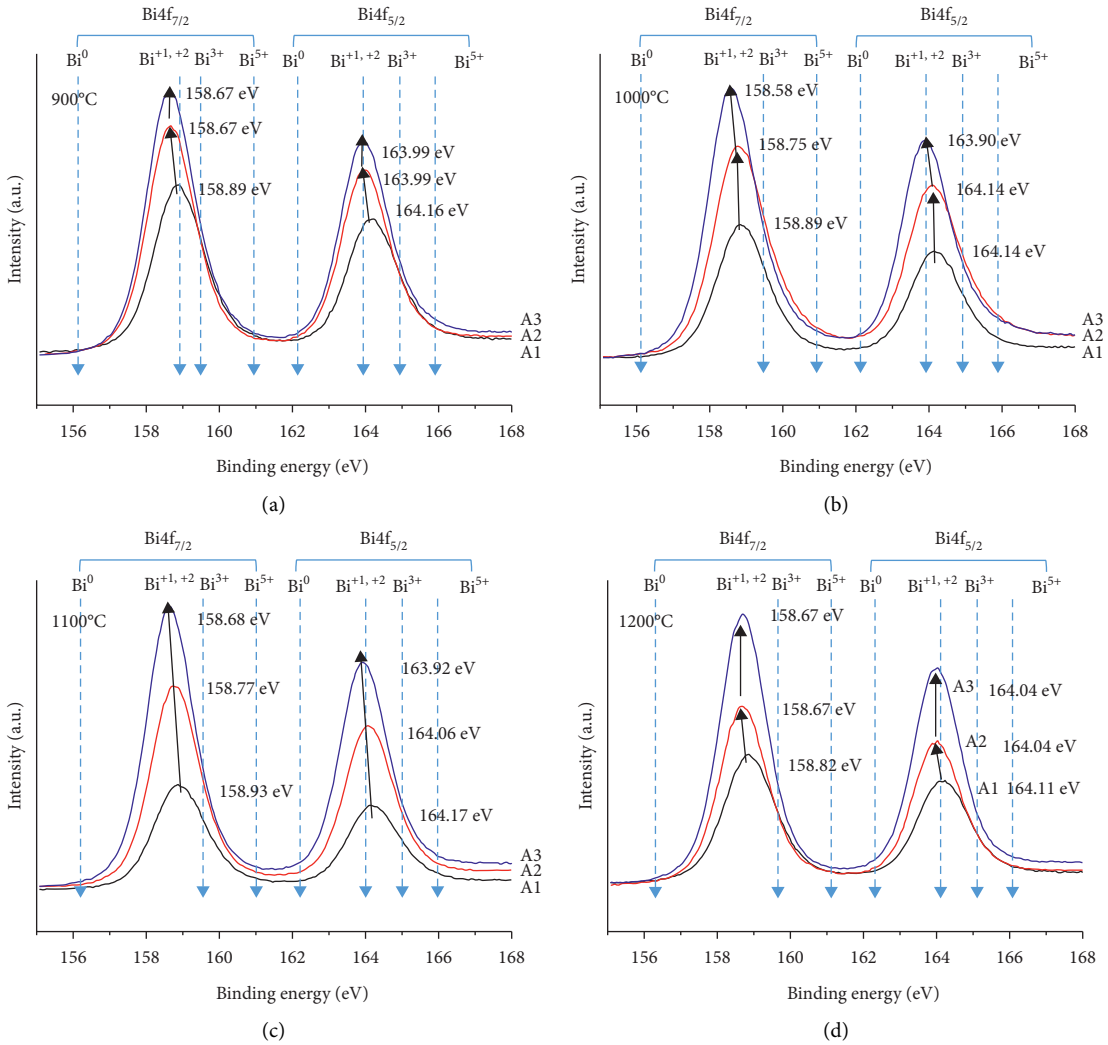

Figure 8: Spectra of Bi4$f_{7/2}$ and Bi4$f_{5/2}$-XPS melted at 900°C, 1000°C, 1100°C, and 1200°C for A1, A2, and A3 series glasses, respectively.

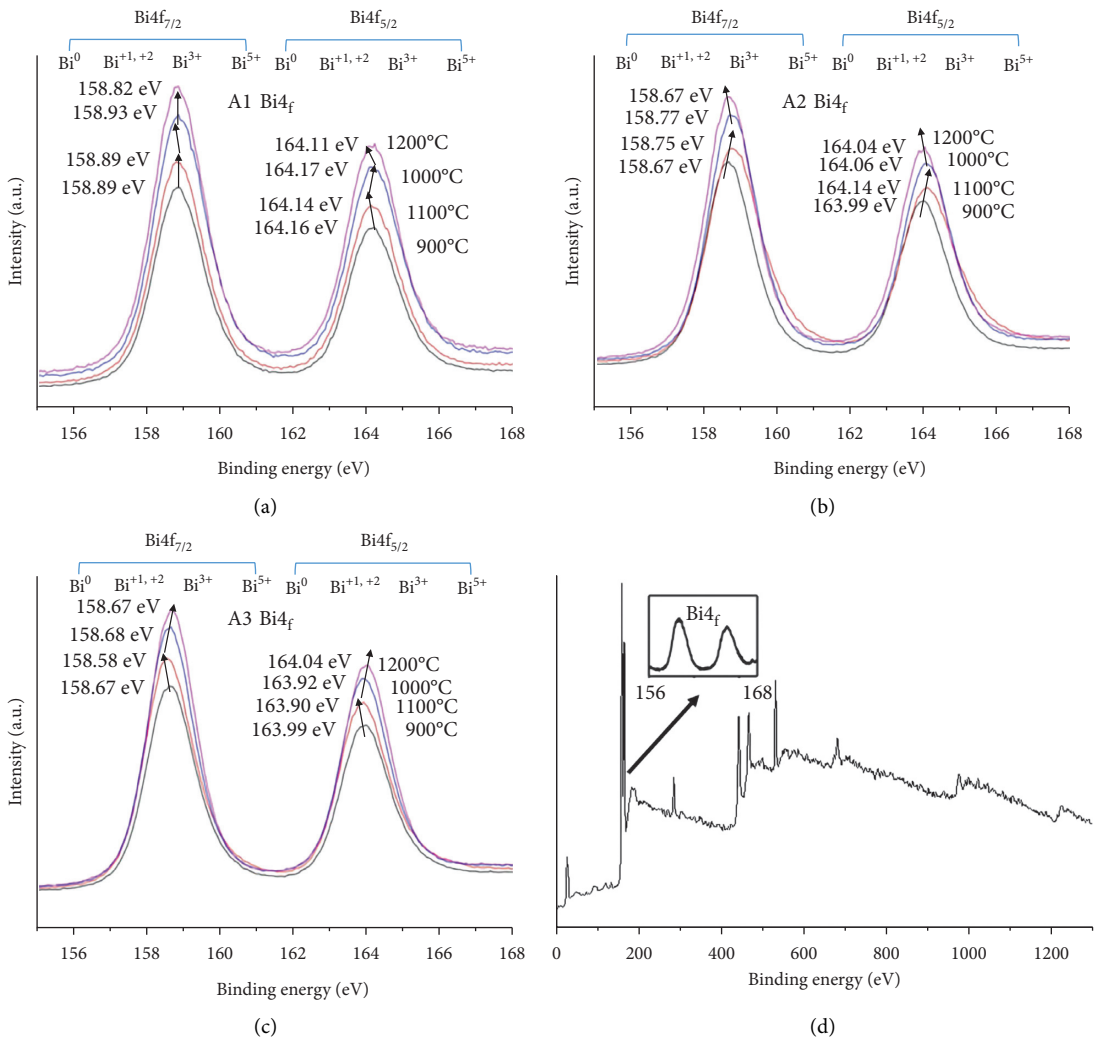

FIGURE 9: Bi4$f_{7/2}$ and Bi4$f_{5/2}$ energy spectra for (a) A1 glass, (b) A2 glass, and (c) A3 glass at different melting temperatures of 900°C, 1000°C, 1100°C, and 1200°C.

melting temperature increases, the energy spectra of Bi4$f_{7/2}$ and Bi4$f_{5/2}$ of A1, A2, and A3 series glass show that, except for the A3 series glass that turns to low energy at 1200°C, the rest tend to shift to high energy direction, which is consistent with the observation results of FTIR.

According to Sanz et al. [28], when the melting temperature is increased from 1050°C to 1300°C by TEM, the particle size of metallic bismuth nanoparticles also changes from 10 nm increasing to 30 nm, the existence of Bi^0 nanoparticles can be found in TEM, and some Bi_2O_3 undergoes thermal reduction, which causes the glass to be colored. Figure 10 shows A series glass test piece. A2 series glass is light yellow at 1000°C, and at 1100°C, it is dark brown, forming a strong contrast.

The O1$_s$, Bi4$f_{7/2}$, and Bi4$f_{5/2}$ energy spectra of A series glass show that with the increase of Bi_2O_3 content, the binding energy of O1$_s$, Bi4$f_{7/2}$, and Bi4$f_{5/2}$ energy spectra shifts to lower binding energy, and with the increase of melting temperature, except for the binding energies of O1$_s$, Bi4$f_{7/2}$, and Bi4$f_{5/2}$ energy spectra of A2 series glasses at 1000°C, the remaining binding energies shift to higher binding energies.

3.4. Thermal Properties of Glass. According to Taisuke Inoue, Tsuyoshi Honma, Vesselin Dimitrov, Takayuki Komatsu, and KH Sun et al. [29, 30], the Zn-O bond strength in the ZnO_4 structural unit is 150.06 kJ/mol, and the Bi-O bond in the BiO_6 structural unit is 102.5 kJ/mol. In this experiment, with the increase of Bi_2O_3 content, the glass XPS energy spectrum (Figure 6) shows the binding energies of O1$_s$, Bi4$f_{7/2}$, and Bi4$f_{5/2}$; except for O1$_s$, Bi4$f_{7/2}$, and Bi4$f_{5/2}$ of A2 series glass at 1000°C, the remaining binding energies all shifted to lower binding energies as the content of Bi_2O_3 increases. And in the FTIR spectrum (Figure 5), the [BiO_3] and [BiO_6] structural units mainly composed of Bi_2O_3 in the glass increase. As the content of Bi_2O_3 increases, the [BO_3] structure concentration increases, the [BO_4] structure concentration decreases, and some B-O-B bonds are bonded with Bi ion to form a B-O-Bi bond with weaker bond energy.

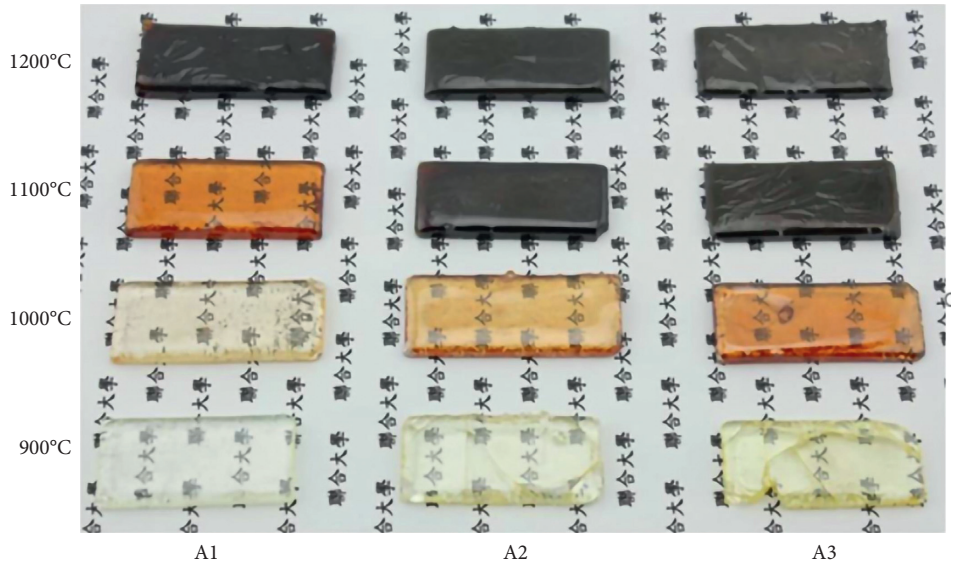

Figure 10: A series glass test piece.

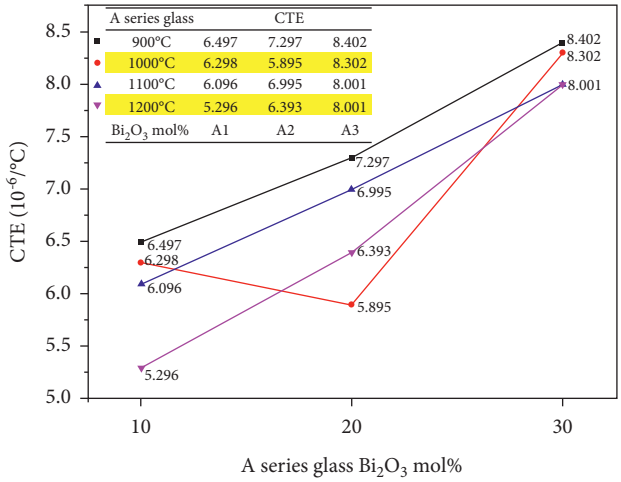

Figure 11: The glass thermal expansion coefficient (CTE) of A series glass observed with Bi_2O_3 content.

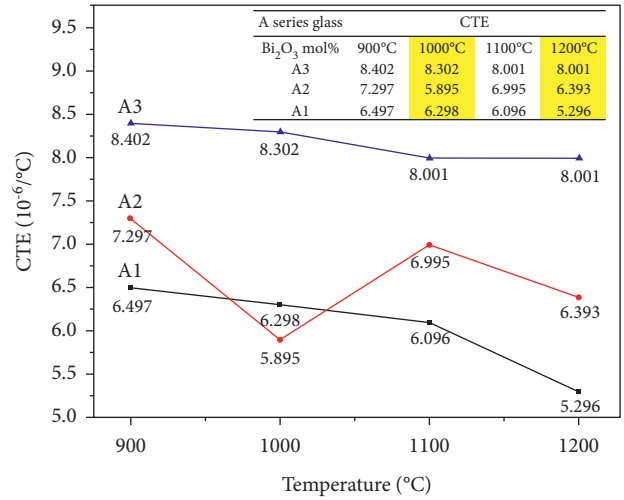

Figure 12: The coefficient of thermal expansion (CTE) of glass A series observed at different melting temperatures.

Figure 11 shows the glass thermal expansion coefficient (CTE) of A series glass observed with Bi_2O_3 content; due to the weaker bond energy of Bi-O-Bi and Bi-O-B, the bond length is longer, and the thermal expansion coefficient increases with the increase of Bi_2O_3 content.

From the literature [29, 30], the structural unit Zn-O bond strength of ZnO_4 is 150.06 kJ/mol, the Bi-O bonding strength in the BiO_6 structural unit is 102.5 kJ/mol, and the bonding strength in B_2O_3 is 497.896 kJ/mole and 372.376 kJ/mole, $BE_B > BE_{Zn} > BE_{Bi}$ (BE, binding energies). Figure 12 shows the glass thermal expansion coefficient (CTE) of A series glass observed at different melting temperatures. The CTE of A2 series glass at 1000°C obviously drops to 5.895×10^{-6}/°C. Figure 7 shows the $O1_s$ spectra of A2; 530.88 eV at 1000°C and 530.68 eV at 1100°C show that the bridging oxygen concentration of A2 at 1000°C is higher than that at 1100°C, and the structural strength of A2 is stronger at 1000°C. Figure 9 shows the $Bi4f_{7/2}$ and $Bi4f_{5/2}$ spectra of A2; $Bi4f_{5/2}$ at 1000°C is 164.14 eV and that at 1100°C is 164.06 eV, and $Bi4f_{7/2}$ at 1000°C is 158.75 eV and that at 1100°C is 158.77 eV, which indicates that the increase of melting temperature leads to the decrease of bridging oxygen concentration of Bi_2O_3, and Bi atoms in $[BiO_3]$ and $[BiO_6]$ tend to be biased toward lower energy B^0 reduction. In FTIR, 700 cm^{-1} and 777 cm^{-1} (dashed arrow) are the vibration signals of the $[BO_3]$ unit. At 1000°C, 700 cm^{-1} is more obvious, indicating that $[BO_3]$ structure concentration is high, $[BO_4]$ structure concentration is slightly smaller, and the 777 cm^{-1} (dashed arrow) signal is weak too. The equilibrium of high binding energy shift shows that the structure and strength of A2 series glass are relatively high when the melting temperature is 1000°C, which means that the A2

series glass structure at the time, with the higher intensity of $[BO_3]$ and $[BO_4]$ structures, has a greater concentration, and the overall structural strength increases, causing the CTE of A2 series glass at 1000°C to drop significantly to 5.895 10^{-6}/°C.

From the straight view of Figure 12, at the melting temperature of 900°C, CTE $_{A1} = 6.497\ 10^{-6}$/°C, CTE $_{A2} = 7.297\ 10^{-6}$/°C, CTE $_{A3} = 8.402\ 10^{-6}$/°C, and CTE increases with the increase of Bi_2O_3 content. From the horizontal view of Figure 12, CTE $_{A1\text{-}900°C} = 6.497\ 10^{-6}$/°C, CTE $_{A1\text{-}1000°C} = 6.298\ 10^{-6}$/°C, CTE $_{A1\text{-}1100°C} = 6.096\ 10^{-6}$/°C, CTE $_{A1\text{-}1200°C} = 5.296\ 10^{-6}$/°C, and CTE decrease as the melting temperature rises, the factor that affects the change of CTE and makes the Bi_2O_3 content change more.

4. Conclusion

In this study, the glass color changed into dark color from transparent yellow with the increase of Bi_2O_3 content and melting temperature, and the dissolution of Bi ions directly affects the color of the glass. The CTE of A2 glass at 1000°C obviously drops to 5.895 10^{-6}/°C, indicating that the glass structure of A2 series glass at this time has a higher concentration of $[BO_3]$ and $[BO_4]$ structural units with higher strength, and the overall structural strength has increased, causing the CTE of A2 series glass at 1000°C drops significantly. And the CTE of glass increases with the increase of Bi_2O_3 content and decreases as the melting temperature rises, the factor that affects the change of CTE and makes the Bi_2O_3 content changes more.

Data Availability

No data were used to support this study.

Conflicts of Interest

The authors declare that there are no conflicts of interest regarding the publication of this study.

Acknowledgments

The authors gratefully acknowledge the financial support of the Ministry of Science and Technology (MOST), Taipei, Taiwan, and The National Sci-Tech Programs: The Study on Manufacture and Sealing Characterization of Bismuth-Zinc Borate Glasses (MOST 103-2221-E-239-005).

References

[1] F. He, J. Wang, and D. Deng, "Effect of Bi_2O_3 on structure and wetting studies of Bi_2O_3-ZnO-B_2O_3 glasses," *Journal of Alloys and Compounds*, vol. 509, no. 21, pp. 6332–6336, 2011.

[2] K. Fajans and N. J. Kreidl, "Stability of lead glasses and polarization of ions," *Journal of the American Ceramic Society*, vol. 31, no. 4, pp. 105–114, 1948.

[3] B. Morten, G. Ruffi, F. Sirotti, A. Tombesi, L. Moro, and T. Akomolafe, "Lead-free ruthenium-based thick-film resistors: a study of model systems," *Journal of Materials Science: Materials in Electronics*, vol. 2, no. 1, pp. 46–53, 1991.

[4] M. Hrovat, T. Maeder, J. Holc, D. Belavič, J. Cilenšek, and J. Bernard, "Subsolidus phase equilibria in the RuO_2-Bi_2O_3-SiO_2 system," *Journal of the European Ceramic Society*, vol. 28, no. 11, pp. 2221–2224, 2008.

[5] S. P. Singh and B. Karmakar, "Bismuth oxide and bismuth oxide doped glasses for optical and photonic applications," *Materials Chemistry and Physics*, vol. 119, no. 3, pp. 355–358, 2010.

[6] G. Gao, L. Hu, H. Fan et al., "Effect of Bi_2O_3 on physical, optical, and structural properties of boron silicon bismuthate glasses," *Optical Materials*, vol. 32, no. 1, pp. 159–163, 2009.

[7] A. Z. Dietzel, "The cation field strengths and their relation to devitrifying processes, to compound formation and to melting points of silicate," *Zeitschrift fuer Elektrochemie*, vol. 48, pp. 9–23, 1942.

[8] S. Bale, S. Rahmana, A. M. Awasthi, and V. Sathe, "Role of Bi_2O_3 content on physical, optical, and vibrational studies in Bi_2O_3-ZnO-B_2O_3 glasses," *Journal of Alloys and Compounds*, vol. 460, no. 68, pp. 699–703, 2008.

[9] M. Imaoka, *Glass-Formation and Glass Structure*, Vol. 7, International Congress on Glass, Brussels, Belgium, 1965.

[10] T. Maeder, "Review of Bi_2O_3-based glasses for electronics and related applications," *International Materials Reviews*, vol. 58, pp. 1–179, 2012.

[11] Y. Huang, Y. Li, J. Wang, M. E. N. G. Zheng, and M. Chang, "Network structures and characteristics of Bi_2O_3–ZnO–B_2O_3 ternary system glasses. China building materials academy, beijing 100024, China," *Journal of the Chinese Ceramic Society*, vol. 43, no. 7, pp. 182–185, 2015.

[12] A. Saitoh, K. Hayashi, K. Hanzawa et al., "Origins of the coloration from structure and valence state of bismuth oxide glasses," *Journal of Non-crystalline Solids*, vol. 560, Article ID 120720, 2021.

[13] K. Gerth and C. Rüssel, "Crystallization of Bi4Ti3O12 from glasses in the system Bi2O3/TiO2/B2O3," *Journal of Non-crystalline Solids*, vol. 221, no. 1, pp. 10–17, 1997.

[14] S. Khonthon, S. Morimoto, Y. Arai, and Y. Ohishi, "Redox equilibrium and NIR luminescence of Bi_2O_3-containing glasses," *Optical Materials*, vol. 31, no. 8, pp. 1262–1268, 2009.

[15] M. Peng, Q. Zhao, J. Qiu, and L. Wondraczek, "Generation of emission centers for broadband NIR luminescence in bismuthate glass by femtosecond laser irradiation," *Journal of the American Ceramic Society*, vol. 92, no. 2, pp. 542–544, 2009.

[16] C.-C. Hsieh and S. Jiin-Jyh, *Addition of B_2O_3 to Improve the Characteristics of SnO-MgO-P_2o_5 Low-Temperature-Sealing Glasses*, Datung University, Taipei, Taiwan, 2007.

[17] R. Iordanova, y. Dimitriev, V. Dimitrov, S. Kassabov, and D. Klissurski, "Glass formation and structure in the $V_2O_5Bi_2O_3Fe_2O_3$ glasses," *Journal of Non-crystalline Solids*, vol. 204, no. 2, pp. 141–150, 1996.

[18] A. Chahine and M. Et-tabirou, "Structural study of (50-x) Na2O-xCuO-10Bi2O3-40P2O5 glasses," *Materials Research Bulletin*, vol. 37, no. 12, pp. 1973–1979, 2002.

[19] E. I. Kamitsos, A. P. Patsis, M. A. Karakassides, and G. D. Chryssikos, "Infrared reflectance spectra of lithium borate glasses," *Journal of Non-crystalline Solids*, vol. 126, no. 1-2, pp. 52–67, 1990.

[20] D. Saritha, Y. Markandeya, M. Salagram, M. Vithal, A. K. Singh, and G. Bhikshamaiah, "Effect of Bi_2O_3 on physical, optical and structural studies of ZnO-Bi_2O_3-B_2O_3 glasses," *Journal of Non-crystalline Solids*, vol. 354, no. 52-54, pp. 5573–5579, 2008.

[21] G. Sharma, K. Singh, S. Manupriya, S. Mohan, H. Singh, and S. Bindra, "Effects of gamma irradiation on optical and

structural properties of PbO-Bi_2O_3-B_2O_3 glasses," *Radiation Physics and Chemistry*, vol. 75, no. 9, pp. 959–966, 2006.

[22] S. Bale, N. S. Rao, and S. Rahman, "Spectroscopic studies of Bi_2O_3-Li_2O-ZnO-B_2O_3 glasses," *Solid State Sciences*, vol. 10, no. 3, pp. 326–331, 2008.

[23] A. K. Hassan, L. Börjesson, and L. M. Torell, "The boson peak in glass formers of increasing fragility," *Journal of Non-crystalline Solids*, vol. 172, pp. 154–160, 1994.

[24] A. A. Kharlamov, R. M. Almeida, and J. Heo, "Vibrational spectra and structure of heavy metal oxide glasses," *Journal of Non-crystalline Solids*, vol. 202, no. 3, pp. 233–240, 1996.

[25] B. N. Meera and J. Ramakrishna, "Raman spectral studies of borate glasses," *Journal of Non-crystalline Solids*, vol. 159, no. 1-2, pp. 1–21, 1993.

[26] R. K. Brow, D. R. Tallant, S. T. Myers, and C. C. Phifer, "The short-range structure of zinc polyphosphate glass," *Journal of Non-crystalline Solids*, vol. 191, no. 1-2, pp. 45–55, 1995.

[27] G. Lin, D. Tan, F. Luo, D. Chen, Q. Zhao, and J. Qiu, "Linear and nonlinear optical properties of glasses doped with Bi nanoparticles," *Journal of Non-crystalline Solids*, vol. 357, no. 11-13, pp. 2312–2315, 2011.

[28] O. Sanz, E. Haro-Poniatowski, J. Gonzalo, and J. M. Fernández Navarro, "Influence of the melting conditions of heavy metal oxide glasses containing bismuth oxide on their optical absorption," *Journal of Non-crystalline Solids*, vol. 352, no. 8, pp. 761–768, 2006.

[29] T. Honma, Y. Benino, T. Komatsu, R. Sato, and V. Dimitrov, "Correlation among electronic polarisability, optical basicity, interaction parameter and XPS spectra of Bi_2O_3-B_2O_3 glasses," *Physics and Chemistry of Glasses*, vol. 43, p. 32, 2002.

[30] K.-H. Sun, "Fundamental condition of glass formation," *Journal of the American Ceramic Society*, vol. 30, no. 9, pp. 277–281, 1947.